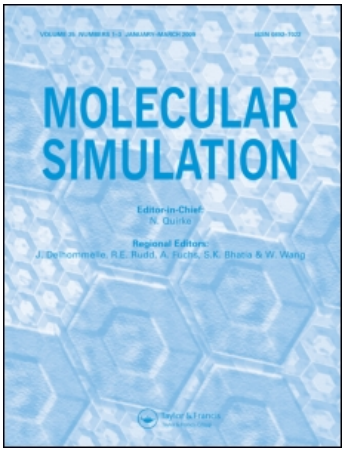

Molecular Simulation

Publication details, including instructions for authors and subscription information:
http://www.informaworld.com/smpp/title~content=t713644482

Generation of Fractal Silicas by Negative Pressure Rupturing of SiO_2 Glass

John Kieffer[a]; C. Austen Angell[a]
[a] Department of Chemistry, Purdue Univeristy, West Lafayette, IN, U. S. A.

To cite this Article Kieffer, John and Angell, C. Austen(1989) 'Generation of Fractal Silicas by Negative Pressure Rupturing of SiO_2 Glass', Molecular Simulation, 3: 1, 137 — 154
To link to this Article: DOI: 10.1080/08927028908034624
URL: http://dx.doi.org/10.1080/08927028908034624

Molecular Simulation, 1989, Vol. 3, pp. 137–154
Reprints available directly from the publisher
Photocopying permitted by license only

GENERATION OF FRACTAL SILICAS BY NEGATIVE PRESSURE RUPTURING OF SiO_2 GLASS

JOHN KIEFFER and C. AUSTEN ANGELL

Department of Chemistry Purdue Univeristy West Lafayette, IN 47907, U.S.A.

(Received March, 1988; in final form September, 1988)

Stimulated by the finding that SiO_2 aggregates (e.g. SiO_2 "smokes" or "snow") assembled under highly non-equilibrium conditions have fractal geometries and dynamics – and retain them under annealing densification almost until the density of silica glass is reached – we have examined the consequences of an inverse procedure. Using the power of molecular dynamics to perform otherwise difficult experiments we have subjected normal density vitreous SiO_2 at 300 K to isotropic expansions (which generate negative pressures) to and well beyond the tensile limit at -70 kbar. As the tensile limit is exceeded, void-containing structures are produced which indeed prove to be fractal in character, and the pressure trends towards zero. The fractal dimension is determined concordantly from two different density correlation relationships and is found to change smoothly with density from 3.0 at the tensile limit down to 1.7 at the limiting density of 0.1 g/cm^3 set by our system size. Our study suggests that the path of least resistance to the rupturing of an initially stable structure may be the path to fractal geometries.

KEY WORDS: Silica, fractal, isotropic expansion, rupture

1. INTRODUCTION

There is a continuing interest in high strength, low weight materials either as composites or as pure materials with controlled void space distributions – for instance, foams, and porous materials produced by condensation or sol-gel processes. Considerable attention has been given recently to porous forms of silica produced by the latter two procedures since the distribution of void space is evidently well-described by the laws of fractal geometry. The densities of silica "smokes" (or aerogels) may be extremely low, e.g. 1/10 the density of vitreous silica, yet they have mechanical stability and hence are candidates for high strength/low weight materials.

Recent studies have demonstrated the existence of fractal geometry in these materials [1,2] and have gone some way towards establishing the validity of the Orbach-Alexander predictions for vibrational dynamics of fractal objects [3,4]. Since we have, for some time, studied the properties of dense random silica and their aluminosilicate analogs at normal (and also high) density using the methods of molecular dynamics [5,6] we have naturally become interested in the possibility of extending such studies to the low density materials.

One of the attractive aspects of the molecular dynamics computer simulation method is the possibility of performing experiments which are extremely difficult to realize in the laboratory. Here we apply this possibility to the silica smoke problem. The normal procedure for producing silica smokes is by non-equilibrium condensation from the vapor. The condensate is then studied at different stages of thermal annealing along the densification path leading to vitreous silica. We thought it would be interesting to investigate the products of an inverse of this procedure. We commence with an equilibrated (non-fractal) vitreous silica sample and subject it to a

rapid isotropic stretching. This procedure instantaneously stretches all the silicon-oxygen bonds 10 to 35% beyond their equilibrium lengths. Beyond a certain point, the tensile (negative pressure) limit for the material, the structure ruptures and the particles rapidly reassemble to reach the nearest mechanical energy minimum.

The resulting structure is then allowed to relax to a stable pressure before its geometry and dynamics are analyzed. This is repeated for different densities, stepping down to a limiting low value set by the size of primary box. (When the mean void size exceeds the box volume the calculations become meaningless). The insight which is gained on the void formation process is very helpful in understanding phenomena related to fracture mechanics and cavitation. The concept of expanding silica network structures in a computer experiment has been seen before in the uniaxial tension fracture studies of simulated SiO_2 reported by T.F. Soules [7] and comments on the relation between our studies will be made later. The important difference and novel feature in the present work is that, rather than completely disintegrating the network, we allow structures at low densities to reach an energy minimum and determine the geometrical characteristics of these metastable configurations.

2. COMPUTATIONAL PROCEDURE

For the computations we used central force pair potentials of the Born-Mayer form with a Verlet algorithm and a full Ewald summation method. The parameters were optimized to match the experimentally determined bond length between silicon and oxygen and the inter-particle distances silicon–silicon and oxygen–oxygen. The configurations were randomized at 6000 K and equilibrated under constant pressure. The configurations were then cooled over 8 to 10 ps using a method described by Andersen [8] to about 2500 K where they assumed a density of 2.16 g/cm^3. In a final step the melts were quenched to 300 K. This last step was performed rather quickly in 1 ps since it was not important to obtain a well equilibrated configuration at this point. These quenched configurations served then as a starting point for the stepwise expansion.

The series of stereoscopic views in Figure 1 shows the arrangement of a system of 300 silicon and 600 oxygen particles at various stages of the expanison. The connecting lines represent silicon–oxygen bonds, satisfying the criteria that bonds exist between Si^{4+} and O^{2-} ions less than 0.21 nm apart, provided that there are not more than three other shorter bonds to the same Si. The important details of the structural modifications are described in the following. Each expansion step is accompanied by a sharp increase in energy and a subsequent decay as the structure relaxes to a more stable state. In Figure 2 two energy peaks for the same relative amount of stretching but for target densities differing by an order of magnitude are compared. The increase of the total energy is composed of a bond bending or stretching affecting the structure only within the range of nearest or second nearest neighbors, and a bond breaking. The latter can be understood as the cooperative response of the local structure to the imposed stresses. Breaking one bond allows the immediately surrounding area to relax momentarily and a small void to open in the structure. This is somewhat analogous to the elastic and plastic deformation in metals, except that the defects introduced in the metal in the form of dislocations are of different nature. The metal can plastically deform without rupturing. The dislocations migrate and new ones develop, until the concentration of dislocations becomes too high and the material

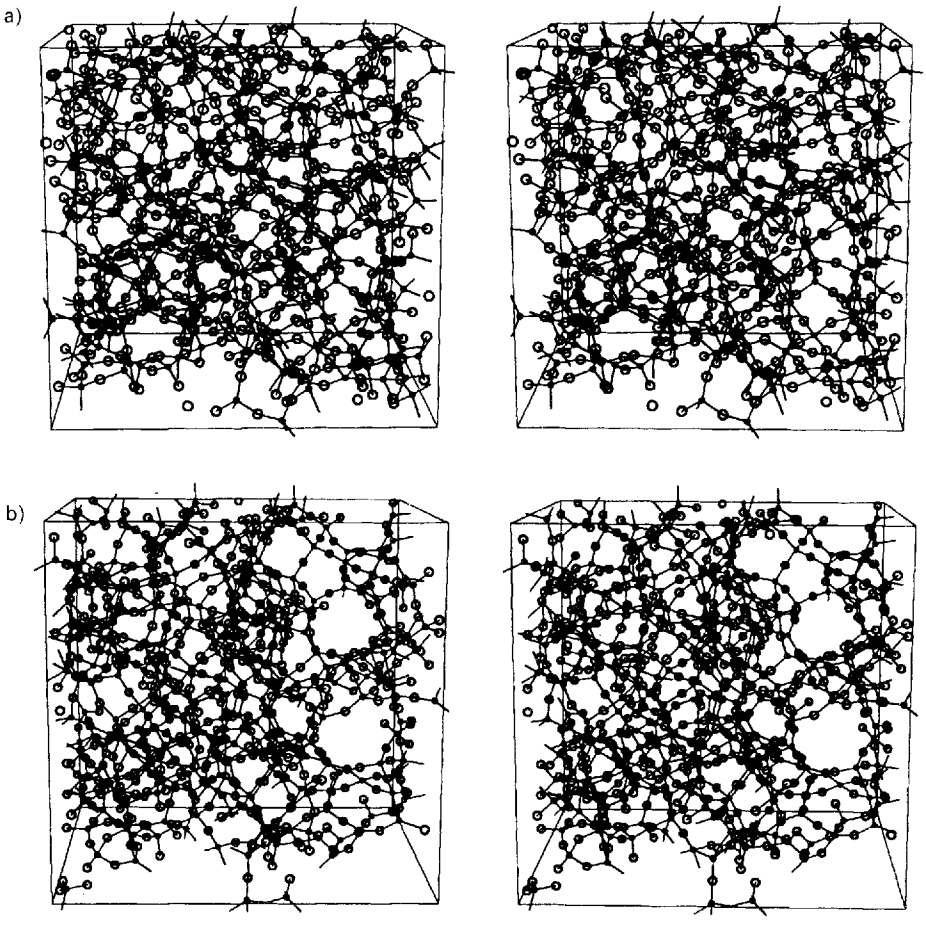

Figure 1 Stereographic views of simulated SiO_2 configurations at various stages of the expansion. The densities are a) $\varrho = 2.16\,g/cm^3$ and b) $\varrho = 1.4\,g/cm^3$. (Note that in order to preserve the stereographic effect, the boxes must have a given size. The fact that each configuration corresponds to a different density is reflected in the varying particle size.)

finally breaks. In an amorphous structure, where no collective behaviour is possible, the defect remains isolated and assumes a different geometry as we will see further down.

In Figure 3 we show the total radial distribution functions for various densities after relaxation. This magnified detail shows the section corresponding to the first and second coordination shells. The peaks corresponding to the pairs of nearest neighbours Si–O, O–O and particularly Si–Si are shifting towards larger distances as the density decreases from 2.16 to 1.6 g/cm^3. The shift in Si–Si distance is indicative of the Si–O–Si bond straightening before the Si–O bonds are obliged to lengthen. Below about 1.6 g/cm^3, which is a critical density (see below), the locations of all peaks superimpose. At these densities bond angle straightening has reached a saturation and the structure changes in a manner that affects only the longer range order, namely by

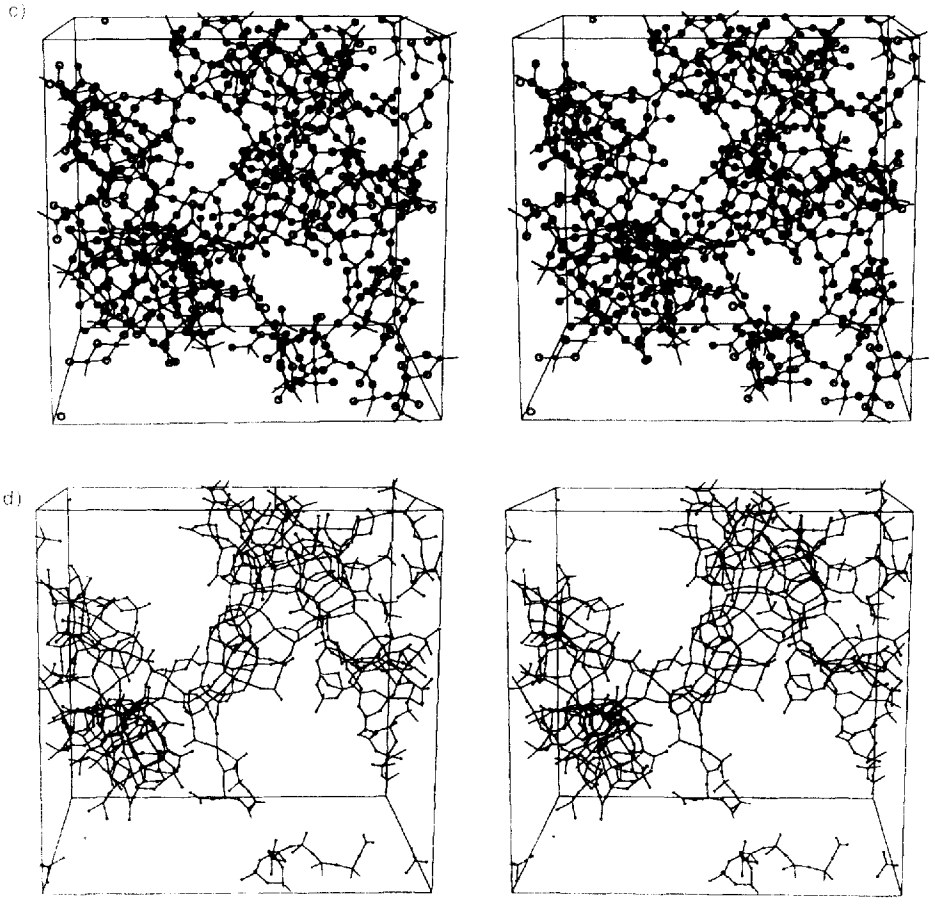

Figure 1 (continued) Stereographic views of simulated SiO_2 configurations at various stages of the expansion. The densities are c) $\varrho = 0.9\,g/cm^3$ and d) $\varrho = 0.5\,g/cm^3$. (Note that in order to preserve the stereographic effect, the boxes must have a given size. The fact that each configuration corresponds to a different density is reflected in the varying particle size.)

opening gaps. Small voids are difficult to recognize as a new feature in the amorphous structure: they become only more apparent as they grow bigger upon further decrease of the density. However, the change is signalled by an abrupt reversal in the variation of the pressure – calculated from the virial as usual – with density as discussed further below. It is important to notice that the voids form at distinct places (nucleation sites) in the structure and remain centered around this original location as they open up. The growth of the voids is of course realized by breaking of bonds in the immediate neighborhood, which shows that the internal surfaces of the voids constitute regions of high energy. Also voids start forming at different locations at different moments during the expansion process and develop at first rather independently. At any given time a broad distribution of void sizes can be found in the configuration. At a more

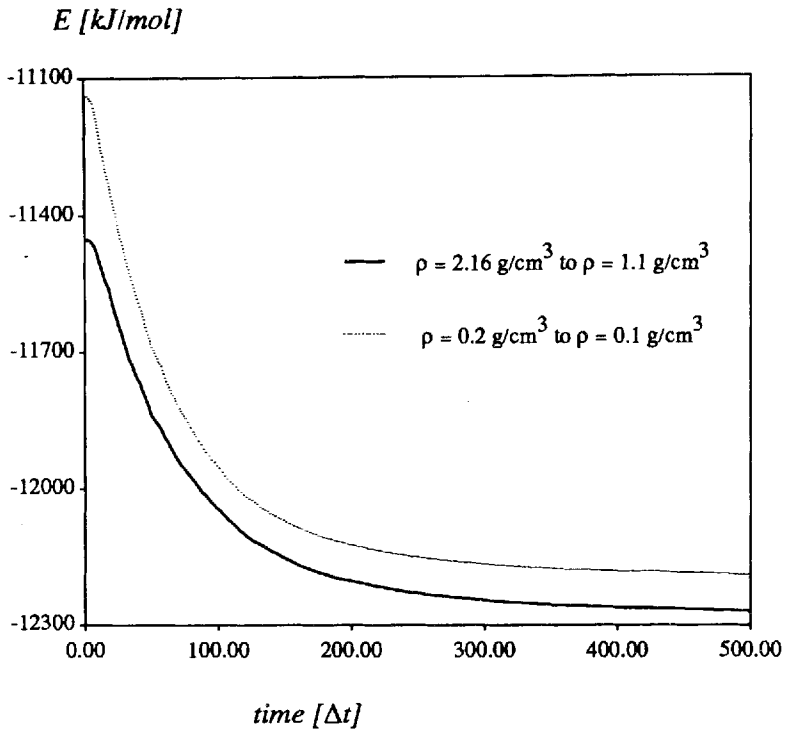

Figure 2 Time development of the total energy of two systems after a step expansion. In both cases the target density is half the initial density; they require approximately the same relaxation time. (Δt = 0.002 ps).

advanced stage of the expansion (Figure 1d), corresponding to densities of about 0.5 g/cm^3, individual voids combine to form larger ones. The silicon and oxygen ions group in a few large clusters linked by tortuous chains. Although the configuration spans the simualtion box in different directions and forms a continuous structure by virtue of periodic boundary conditions, the structure has gradually lost connectivity in the higher dimensions. Below densities of 0.2 to 0.3 g/cm^3 the connectivity disappears completely, such that a continuous sequence of bonds connecting any particle to its own images in the periodic reproductions of the simulation box can no longer be found. After the last bonds that established percolation through the network have broken, the chainlike extensions of the clusters recoil. Under conditions of constant pressure, where the density is free to adjust, the density increases about 20% and then remains stable. The development of ramified structures in the later stages of rupture is similar to results demonstrated by Soules for the rupture of silica "rods" in uniaxial tension. Soules and Busbey [7] even found a similar tensile stress, being $\sim$ 50 kbar in their case.

We have simulated configurations with total number of particles of 300, 600, 900, 1200 and 1500 particles. The percolation threshold seems to be independent of the number of particles within this range and it is also independent of the rate of

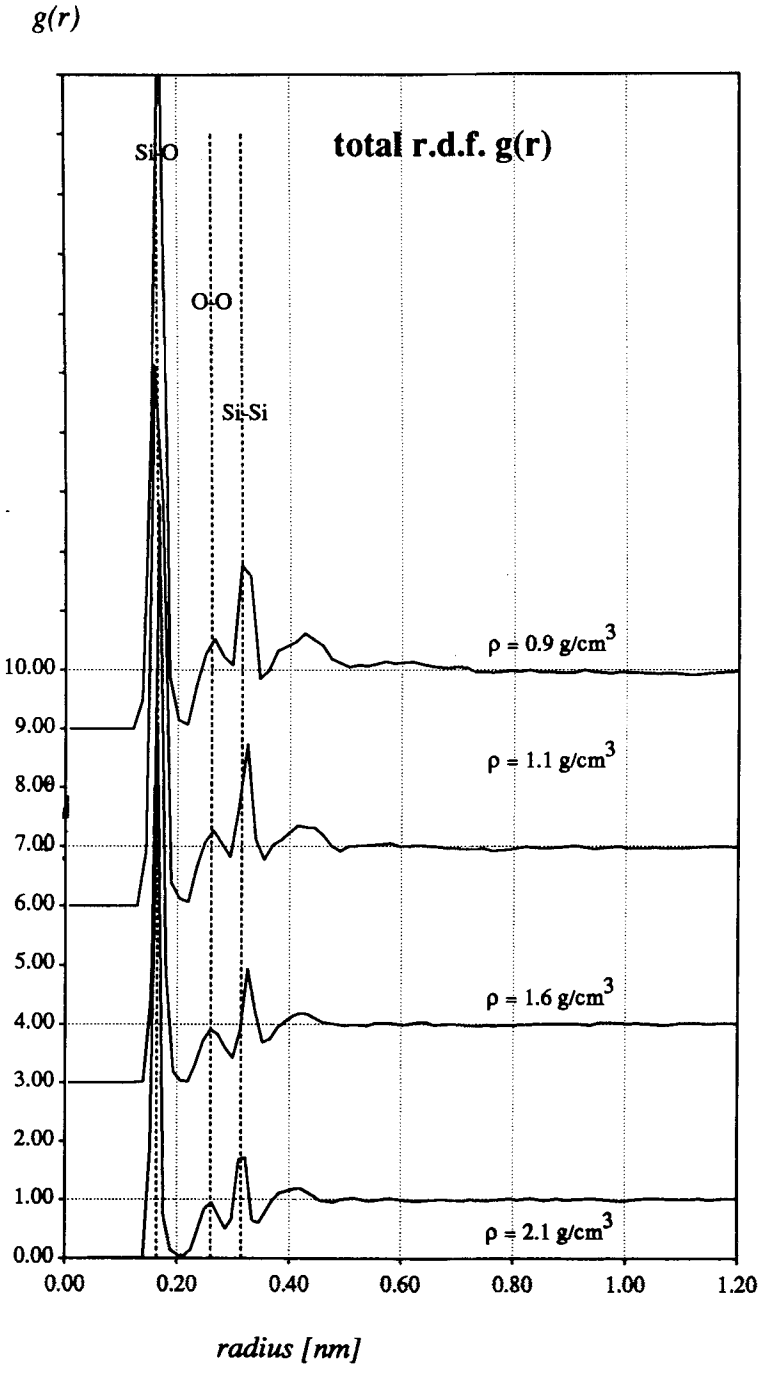

Figure 3 Total radial distribution functions for silica configurations at 300 K (after relaxation) for the initial steps of expansion from the normal density.

expansion. Usually, the expansion was performed in steps of 0.4 g/cm^3 for the higher densities and in steps of 0.1 g/cm^3 for densities below 1.0 g/cm^3. On the other hand, if an expansion is simulated that takes the configuration in a single step from 2.16 g/cm^3 to a target density below the percolation threshold, the structure has ruptured and a few isolated clusters form. If however, the target density is still above the percolation threshold, all particles reassemble in a single structure that spans the simulation box. Naturally the time necessary to equilibrate after a large density jump is much longer. The physical situation which is established in this case is different in that all interparticle distances have been rescaled instantaneously far beyond any stable bond length. The mobility of the dispersed particles is drastically increased as they are taken out of their local potential well and the reassembly process is much like a diffusion limited aggregation (DLA). At first short linear chains form which then agglomerate to form larger clusters that are interconnected. A systematic comparison of the structures that result from a gradual or catastrophic expansion will be given in the following section. The number of clusters that form by the time the configuration has been taken below the percolation threshold density depends on the system size. One cluster usually includes several hundred particles. A more accurate determination of a cluster size distribution seems inappropriate due to the poor statistics even with systems of 1500 particles.

3. GEOMETRIC ASPECT-THE FRACTAL DIMENSIONS

The tortuous appearance of the chains connecting isolated clusters, the existence of voids of all sizes and the gradual loss of connectivity in higher dimensions suggests that the structure of these low density silica aggregates scales according to a fractal dimension. In the following we conduct a simple test to verify this suspicion and determine the numerical value for the fractal dimension of a particular structure from radial distribution functions (a technique which should be fairly comprehensible for a person versatile in molecular dynamics simulation techniques).

We start out by recalling the definition of a dimension d based on the concept of capacity or "box-counting" dimension given by

$$d = \lim_{\varepsilon \to 0} \frac{ln\, N(\varepsilon)}{ln(l/\varepsilon)}, \tag{1}$$

where N is the number of entities that compose the system and ε is the resolution that can be applied to examine the system. In our case it is easy to think of the entities as being atoms or ions. Equation (1) is also equivalent to

$$N(l/\varepsilon) \propto \left(\frac{l}{\varepsilon}\right)^{d} \tag{2}$$

As we count the number of entities as a function of the distance form an arbitrary point, measured in multiples l of the resolution ε, the number will be proportional to this distance raised to a power d, the dimension of the object. For any regular object d will be the dimension of the underlying Euclidian space. It is however less than the dimension of the Euclidian space in case of fractal objects and we have to formally replace d in Equation (2) by d_f, the Hausdorff dimension. If we substitute r for l/ε and reformulate Equation (1) as a derivative, we get as a definition for the dimension d_f:

$$d_f = \frac{d \ln N(r)}{d \ln r} \tag{3}$$

In Figure 4 we have plotted the number of ions surrounding a central one $N(r)$ as a function of distance in a double logarithmic scale. The different curves correspond to different densities. The interesting part in the present context is the range of distances

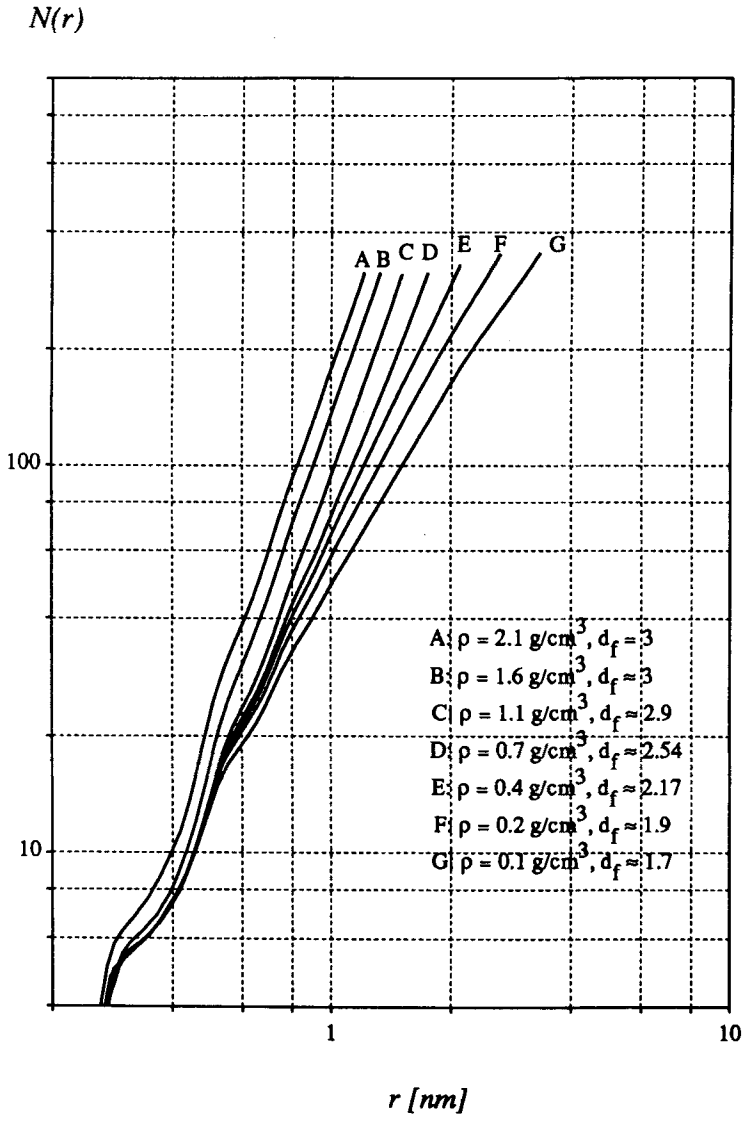

Figure 4 Number of ions N(r) that can be found within a sphere of radius r centered at an arbitrary point in the configuration for various densities. The slopes yield the fractal dimension d_f.

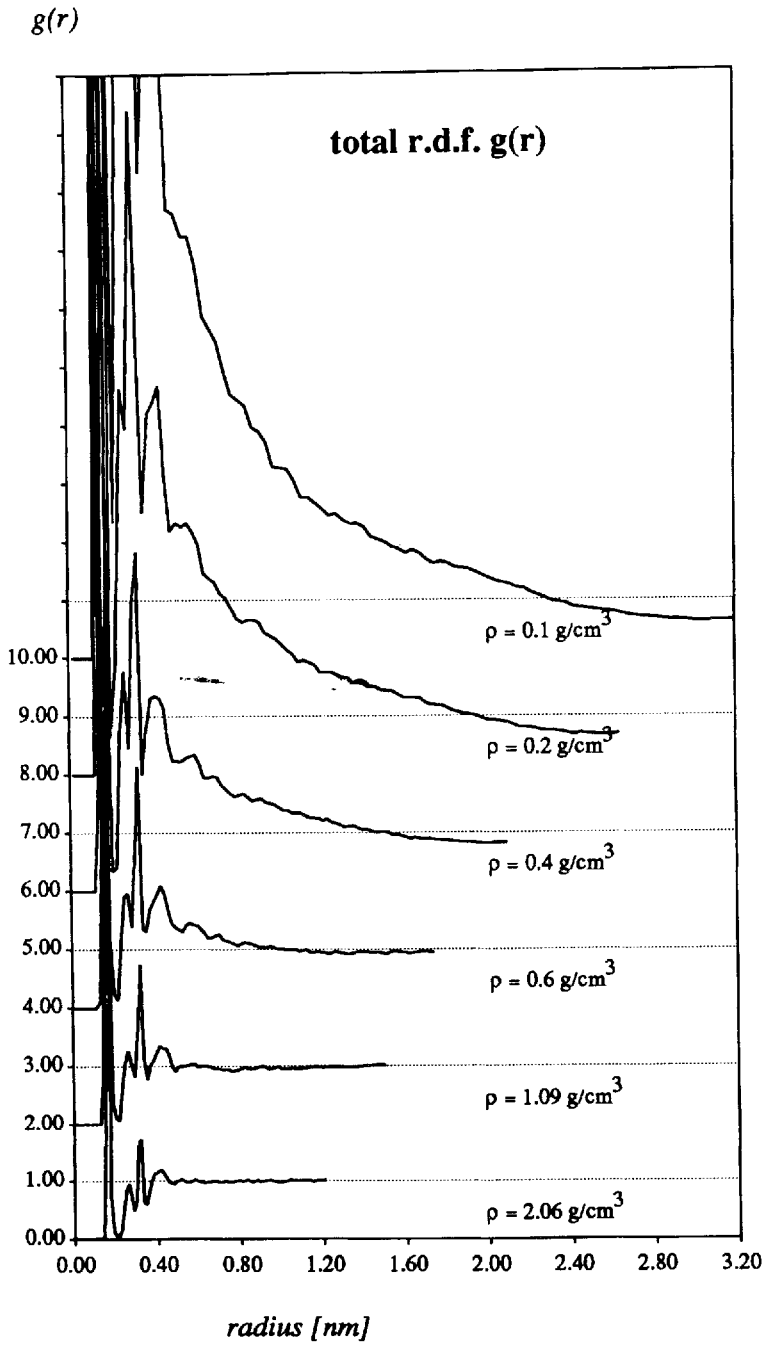

Figure 5 Normalized total radial distribution functions for various densities of simulated SiO_2 at 300 K.

above 0.5 nm, i.e. the region beyond the second coordination shell. These parts of the curves can be well approximated by a straight line and the slope gives the numerical value of the fractal dimension d_f.

It is now very straightforward to relate the fractal dimension d_f to the radial distribution function $g(r)$ by using its definition, given by the relation

$$\frac{dN(r)}{dr} = 4\,\pi\, r^2 \varrho_0\, g(r) = Y, \tag{4}$$

in Equation (3) to yield

$$d_f = \frac{d\ln N(r)}{d\ln r} = \frac{r \cdot Y}{N(r)} \tag{5}$$

or

$$d_f \cdot N(r) = r \cdot Y \tag{6}$$

Taking the derivative with respect to r of both sides of the equation, assuming that d_f is constant over the range of r considered yields

$$d_f \cdot \frac{dN(r)}{dr} = Y + r \cdot \frac{dY}{dr}. \tag{7}$$

Substituting Equation (4) in Equation (7) gives

$$(d_f - 1) \cdot Y = r \cdot \frac{dY}{dr} = 2Y + r \cdot \frac{d\ln g(r)}{dr}. \tag{8}$$

And after some rearranging we finally obtain the desired relation

$$d_f = 3 + \frac{d\ln g(r)}{d\ln r} \tag{9}$$

Now the dimension of a given structure is equal to the dimension of the underlying Euclidian space, which is 3, plus the value of the slope of the logarithm of the normalized radial disstribution function vs. the logarithm of the distance. Figure 5 reveals even more detail. In this figure the normalized radial distribution functions g(r) for configurations with densities ranging from the normal 2.16 g/cm^3 down to 0.1 g/cm^3 are plotted. Apart from the adjustment in the short range order as pointed out in the previous section (i.e., the straightening of Si–O–Si bonds), another feature becomes noticeable in the radial distribution functions at lower densities: the initial sharp spikes, which still reflect the nearest neighbour order, are succeeded by a slow power-law decay preceding the levelling out to a horizontal. This is the range of distances where Equation (8) applies. In the log–log plot seen in Figure 6, the power-law tails are linearized and the fractal dimensions d_f are obtained from the slopes according to Equation (9). For low densities the linear branches have a negative slope and the values for d_f obtained necessarily agree with those taken from Figure 4.

In the ways the structure of SiO_2 responds to the imposed tensile stresses we can differentiate between the initial stretching of Si–O–Si bonds and later the presence of voids of all sizes as reflected by the fractal geometry of the structure. During the stretching phase, the stress increases in magnitude until it reaches the tensile limit, and

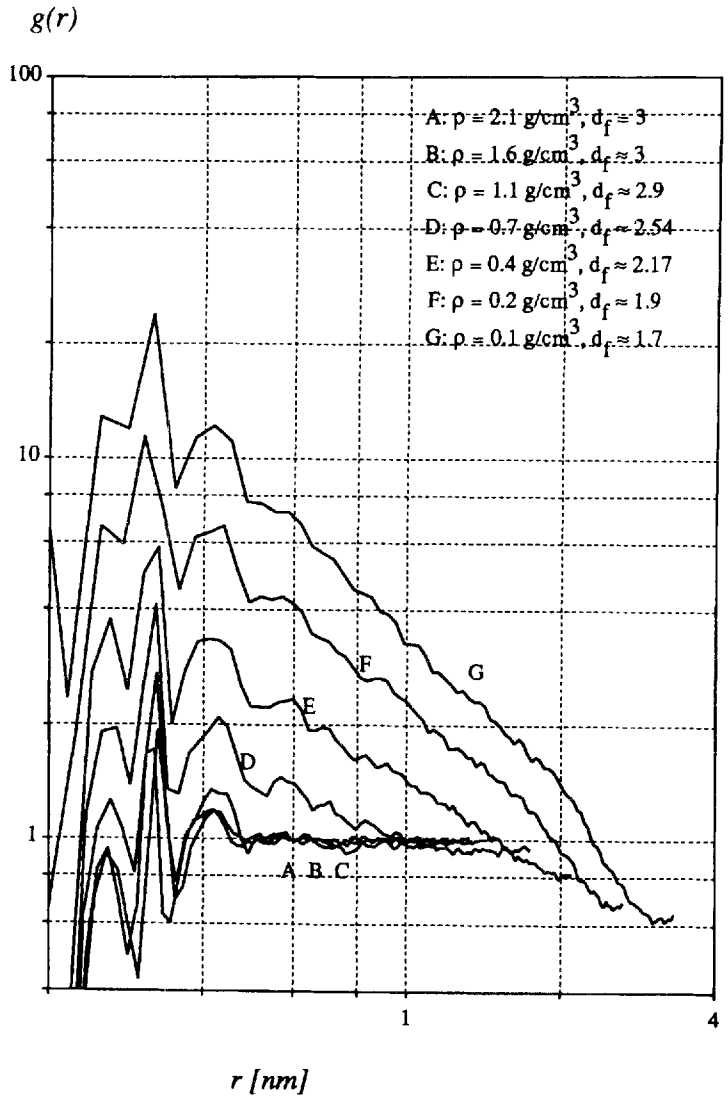

Figure 6 Log–log plot of the total radial distribution functions for various densities of simulated SiO_2 at 300 K.

decreases again when larger voids open. This behavior is shown in Figure 7a where the pressures of the simulated systems are plotted versus their density. It is intriguing to observe that during the expansion, the density where the tensile limit is passed (at -70 kbar) coincides with the onset of fractality for the geometric description of the structures. In other words the path of least resistance to the rupturing of an initially mechanically stable structure is the path to fractal geometries. After an abrupt increase in energy at the point of rupture a new regime of almost density independent

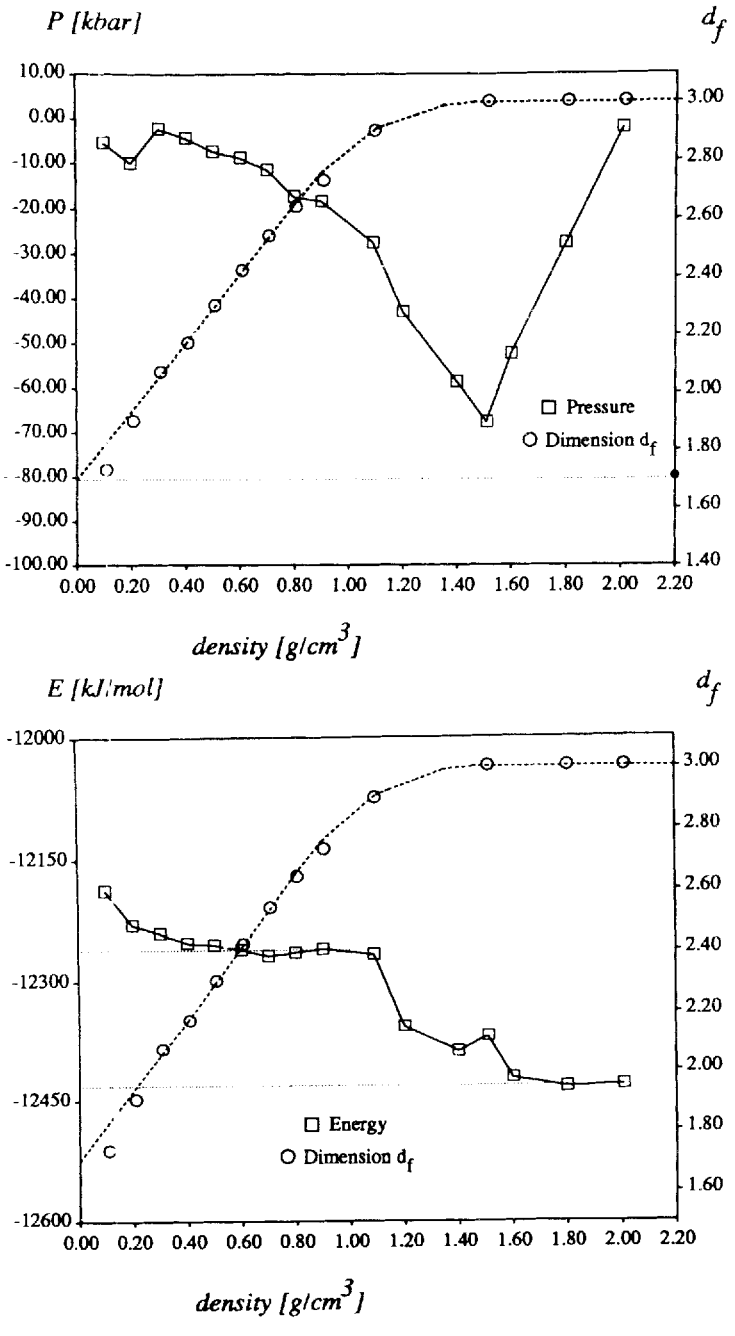

Figure 7 Fractal dimension d_f as a function of the density compared to a) the pressure, b) the total energy.

energy is reached (Figure 7b). We note that the energy gap between these two regions is approximately 150 kJ/mol, which is a small energy relative to the quasi lattice energy of 12450 kJ/mol but rather larger than the calorimetrically determined 46 kJ/mol for the energy difference between vitreous silica and vapor deposited silica "snow" [9]. The latter have fractal dimensions of 2.2–2.4 [1,2] comparable with the value we find at the fractal plateau.

For the densities of 0.2 and 0.1 g/cm^3 the tails of the radial distribution functions have a slightly steeper slope just before they level off horizontally. There is of course

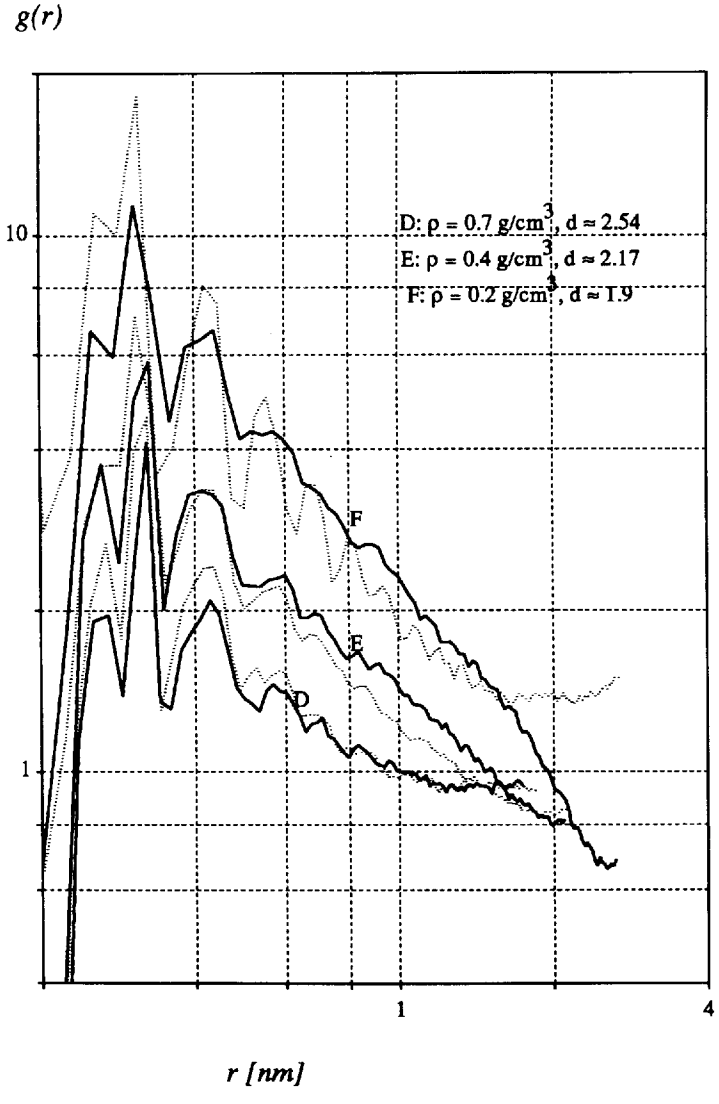

Figure 8 Comparison of radial distribution functions of SiO_2 configurations at various densities. The solid line was obtained by a series of stepwise expansions with intermediate relaxations, while the dotted line shows the results of an abrupt expansion with relaxation only at the target density (DLA).

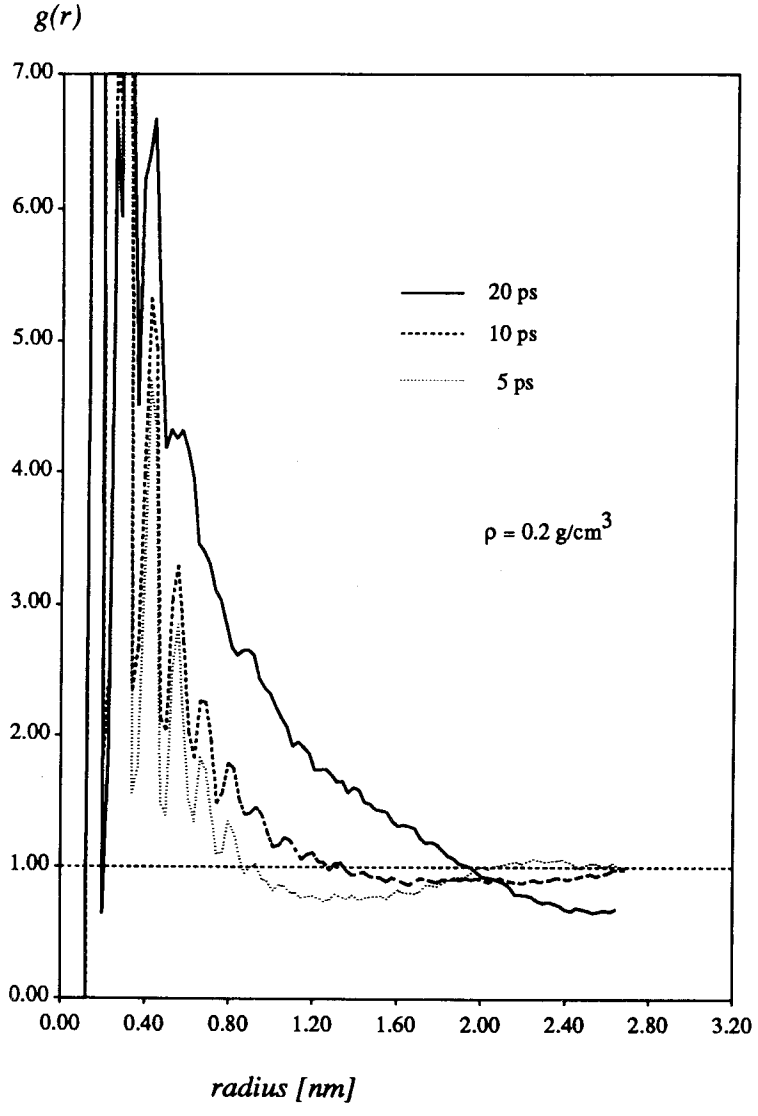

Figure 9 Radial distribution functions of SiO_2 with a density of 0.2 g/cm^3 obtained by an abrupt expansion (DLA) at different stages of the relaxation.

the possibility that different fractal dimensions reign on different length scales, but a more likely explanation is that we are looking at a cutoff effect. Imposing periodic boundary conditions on the simulation box naturally limits the possible range of the fractal dimension. The identical configuration fills all neighboring boxes, next neighbors and so on, this way filling the three dimensional space continuously. Consequently, the range in which structures scale according to fractal dimensions is limited on its high end by the size of the simulation box and on its low end by the

interatomic distances. We believe the extrapolation of d_f to 1.7 at vanishing density to be significant and predictable, but will defer discussion until more detailed studies have been completed.

With Equation (5) and (9) we have the means to quantitatively describe an important characteristic of network structures: their fractal dimension and the range of lengths over which it applies. As indicated in the previous section, we have generated configurations with a certain low target density in two manners. On one hand we expanded it stepwise; in anyone of these expansion steps the Si–O bond distances are stretched between 10 and 35% of their equilibrium length. This leaves the particles sufficiently close to their previous equilibrium position so they will seek the same coordination as they had before. Voids are opened gradually. In a separate series of runs we expanded systems in a single step from their equilibrium configuration at 2.16 g/cm^3 to the target density, i.e. 0.6, 0.4 and 0.2 g/cm^3. In Figure 8 the radial distribution functions for the configurations resulting from either expansion method are compared. They are in good agreement. The curves corresponding to the single step expansion (dotted lines) tend to be lower, especially for the densities close to the percolation threshold; however their slopes are the same within the experimental error. Consequently, these structures scale according to the same fractal dimension, only the range of validity is slightly different. This could be due to the fact that these configurations have not fully relaxed. A typical development of the radial distribution function is shown in Figure 9. The long time convergence demonstrated here indicates that under the same thermodynamic constraints any structure tends towards a metastable state which is described by a unique radial distribution function, and hence a unique fractal regime.

4. DYNAMIC ASPECTS

The molecular dynamic simulation of stable and reproducible fractal network structures is an important step in the investigation of highly disordered materials. Use of numerical simulation techniques allows us to vary thermodynamic parameters as needed and provides a convenient method to determine the mechanically most stable structures. On a fractal not only the mass will scale according to a non-integer dimension, but other properties as well. A theoretical model has recently been proposed by Alexander and Orbach [10] and independently by Rammal and Toulouse [11] that predicts that the density of states for low frequency modes will scale according to

$$\varrho(\omega) = \omega^{\frac{d_f}{\alpha} - 1} \tag{10}$$

where d_f is the Hausdorff fractal dimension of the structure and α a constant particular to the type of fractal. One also refers to $\bar{d} = d_f/\alpha$ as the intrinsic "fracton" dimension.

Having now generated fractal structures via computer simulations it seems natural to use the same technique to determine the density of states for the acoustic modes. This can be done by Fourier transformation of velocity autocorrelation functions. However, a variety of difficulties obstruct a clear interpretation of these results and more detailed studies than we have performed to date will be required. The minimum frequency value is again limited by the extent of the simulation box. This is particular-

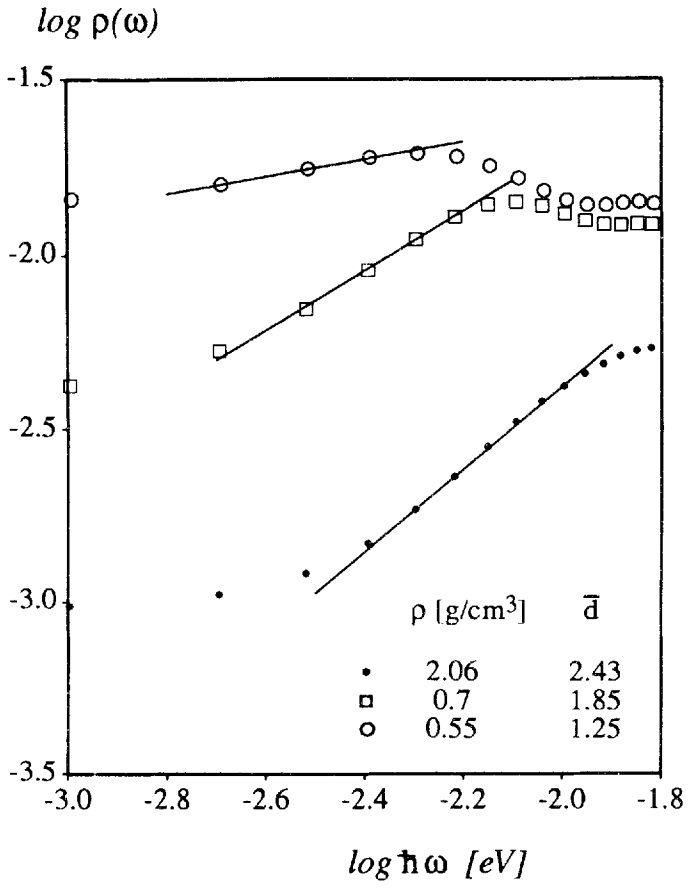

Figure 10 Density of states for three different mass densities at 300 K, obtained from molecular dynamic simulations. The "fracton" dimension describing the vibrational excitations is obtained from the slope of the ascending side of the first (acoustic) peak in this log–log representation.

ly important cosidering the use of periodic boundary conditions: any wave front propagating through the box and arriving at one side will reenter the box at the opposite side and progress on. Therefore it would not be possible to observe a wave with a wavelength longer than the dimensions of the box. Also, structures which are not completely equilibrated still undergo adjustments that appear as diffusive motion and cause a non-zero intersection at zero wavenumbers for the density of states obtained from the velocity correlation functions.

In Figure 10 the first (low-frequency) peak of the density of states is plotted on a log–log scale for three different mass densities. Due to the representation the peaks are broadened and flat, but it can be seen that their maximum is shifted towards lower frequencies with decreasing density. From the examples given in Figure 10 the power law scaling behavior of the density of states becomes obvious: the fracton dimension $\bar{d}$ can be determined from the slope ($=\bar{d}$-1) of the ascending side of this peak and is

found to be directly correlated to the dimension d_f of the structure. Studies being described in more detail elsewhere [12] indicate that at low densities the magnitudes of the Hausdorff and fracton dimension differ by a fairly constant value, the fracton dimension being about 33% smaller than the Hausdorff dimension.

CONCLUDING REMARKS

By analyzing highly irregular structures for their fractal dimension as described in this paper, a fairly simple parameter is obtained for the characterization of these materials. The importance of the fractal dimension results from the correlation with thermodynamic properties, such as pressure, energy and vibrational excitations, which we are only beginning to recognize.

The present studies have all been carried out on SiO_2 because of the availability of experimental data with which to compare the findings. However the results are believed to be of broader significance. There is every reason to believe, for instance, that water, the tetrahedral network character of which is well recognized, will fracture under tensile stress in the same manner as we have observed here for SiO_2. There will be a fractal regime separated by an energy gap from the stretched (negative pressure) state. The difference is that in the conditions of interest in the case of water e.g. in the cavitation at the trailing edge of a ship's propellor, water is in the liquid state, and the transition to the fractal state will be transitory. It seems quite likely to us that it is the release of the "fractal gap" energy, as microscopic fractal regions collapse back to the normal state, that is the source of the damage incurred by a ship's propellors in high speed service conditions. Clearly, it will be of interest to examine the extension of the present study to liquids and glasses of different atomic level structures to discover how general the various findings of this study might be.

Acknowledgements

This work was supported by the National Science Foundation Grant No. DMR 8304887. We wish to acknowledge the role of Prof. L.M. Torell of Chalmers University of Technology, Gøthenburg, in alerting us to the importance of this problem.

References

[1] S.R. Forrest and T.A. Witten, "Long-range correlation in smoke-particle aggregates", *J. Phys.* **A12,** L109 (1979).
[2] T. Frelthoft, J.K. Kjems and S.K. Sinha, "Power correlations and finite-size effects in silica particle aggregates studied by small-angle neutron scattering", *Phys. Rev.* **B33,** 269 (1986).
[3] T. Freltoft, J. Kjems and D. Richter, "Density of States in Fractal Silica Smoke-Particle Aggregates", *Phys. Rev. Lett.* **59,** 1212 (1987).
[4] E. Courtens, J. Pelous, J. Phalippou, R. Vacher and T. Woignier, "Brillouin-Scattering Measurements of Phonon-Fracton Crossover in Silica Aerogels", *Phys. Rev. Lett.* **58,** 128 (1987).
[5] L.V. Woodkock, C.A. Angell and P. Cheeseman, "Molecular dynamics studies of the vitreous state: Simple ionic liquids and silica", *J. Chem. Phys.* **65,** 1565 (1976).
[6] C.A. Angell, P.A. Cheeseman and C.C. Phifer, "Dynamics of compressed and stretched liquid SiO_2 and the glass transition", *Mat. Res. Soc. Symp. Proc.* **63,** 85 (1986).
[7] T.F. Soules and R.F. Busbey, "The rheological properties and fracture of a molecular dynamic simulation of sodium silicate glass", *J. Chem. Phys.* **78,** 6307 (1983).

[8] H.C. Andersen, "Molecular dynamic simulation at constant pressure and/or temperature", *J. Chem. Phys.*, **72,** 2384 (1980).
[9] M. Huffman, A. Navrotsky and F.S. Pintchovski, "Thermochemical and Spectroscopic Studies of Chemically Vapor Deposited Amorphous Silica", *J. Electrochem. Soc.*, **133,** 164 (1986).
[10] S. Alexander and R. Orbach, "Density of states on fractals: «fractons»", *J. Physique Lettres* **43,** L-625 (1982).
[11] R. Rammal and G. Toulouse, "Random Walks on Fractal Structures and Percolation Clusters", *J. Physique Lettres* **44,** L-13 (1983).
[12] J. Kieffer and C.A. Angell, "Generation of Fractal Structures by Negative Pressure Rupturing of SiO_2", submitted to *J. Non-Cryst. Sol.*